Vrije Universiteit Brussel

Ammonia-Hydrogen Blends in Homogeneous-Charge Compression-Ignition Engine

Pochet, Maxime; Truedsson, Ida; Foucher, Fabrice; Jeanmart, Hervé; Contino, Francesco

Ammonia-Hydrogen blends in Homogeneous-Charge Compression-Ignition Engine

Maxime Pochet, Ida Truedsson, Fabrice Foucher, Hervé Jeanmart, Franesco Contino

Université catholique de Louvain, Belgium
Université d'Orléans, France
Vrije Universiteit Brussel, Belgium

Abstract

Ammonia and hydrogen can be produced from water, air and excess renewable electricity (Power-to-fuel) and are therefore a promising alternative in the transition from fossil fuel energy to cleaner energy sources. An Homogeneous-Charge Compression-Ignition (HCCI) engine is therefore being studied to use both fuels under a variable blending ratio for Combined Heat and Power (CHP) production. Due to the high auto-ignition resistance of ammonia, hydrogen is required to promote and stabilize the HCCI combustion. Therefore the research objective is to investigate the HCCI combustion of varying hydrogen-ammonia blending ratios in a 16:1 compression ratio HCCI engine, with a specific focus maximizing the ammonia proportion as well as on the NO_x emissions that could arise from the nitrogen contained in the ammonia. A single-cylinder, constant speed, HCCI engine has been used with an intake pressure varied from 1 to 1.5 bar and with intake temperatures ranging from 428 to 473 K. Stable combustion was achieved with up to 70 %vol. ammonia proportion by increasing intake pressure to 1.5 bar, intake temperature to 473 K, and equivalence ratio to 0.28. From pure hydrogen to 60 %vol. ammonia proportion, the combustion efficiency only lost 0.6 points. Pure hydrogen Indicated Mean Effective Pressure (IMEP) was limited to 2.7 bar to avoid ringing (i.e. too high pressure rise rate) but blended with ammonia the IMEP safely reached 3.1 bar. For pure hydrogen, NO_x emissions were below 6 ppm. For hydrogen-ammonia blends, NO_x were between 1000 and 3500 ppm. Exhaust Gas Recirculation (EGR) operations significantly reduced NO_x emissions through a reduced oxygen availability but with a noticeable negative effect on combustion efficiency due to lower in-cylinder temperatures. The performed simulations showed the production of significant N_2O quantities under 1400 K. Ammonia showed to be an effective fuel for HCCI conditions and EGR revealed itself as a promising NO_x reducing technique through a decreased oxygen availability. Still the combustion temperature must be kept above 1400 K

Introduction

Motivation of the work

As the renewable energy production increases to meet the CO_2 emissions reduction goal, the need for electricity storage has never been so high. This storage has various purposes such as balancing the electricity network [1, 2], providing flexibility, hence decreasing the need for back-up fossil fuel energy sources [3, 4], increasing the renewables utilization factor and allowing for more units to be incorporated into the network [5, 6]. As more renewable energy is produced, short-term (daily) storage is not sufficient to balance the grid and absorb excess production. Therefore, mid-term (weekly) and long-term (monthly to yearly) storage are needed if we ever want to achieve a major renewable share in our energy consumption.

Several technologies like hydro-pumping, compressed air storage, and power-to-fuel can be used for mid- and long-term storage [2]. Despite its lower efficiency, power-to-fuel shows a tremendous opportunity giving its much lower CAPEX (capital expenditure) for storage capacity, lower levelized cost of energy and installation constraints than the other long-term storage technologies [7, 8, 9]. This study focuses on hydrogen and ammonia storage fuels whose production and use can be fully decentralized and sustainable: they only require water and nitrogen to be produced from electricity and their combustion products in ideal conditions are water and nitrogen. Hydrogen is obtained from the electrolysis of water with an efficiency of about 70%, based on its Lower Heating Value (LHV), for commercialized alkaline electrolysers. Yet hydrogen is not convenient for storage given its very low energetic density of about 10 kJ/l in normal conditions. To improve its storage density, many solutions exist and are recapitulated in Table 1. These storage routes greatly impact the overall efficiency and the obtained properties are not always desirable: the energetic density of compression storage is rather low; the liquefaction storage has a low efficiency; organic liquid and metal hydrides are expensive and require a specific process to set hydrogen free. Therefore compressed hydrogen is preferred, but only up to mid-term (weekly) storage.

Table 1. Comparison of various hydrogen storage technologies

Hydrogen storage technology	Pressure / Temperature state	Energy density (GJ/m3)	Overall efficiency (LHV)	Storage duration/ capacity
Compressed [10,11]	700 bar / 293 K	4.5	59 %	medium
Liquefied [11,12]	1 bar / 20 K	8.5	49 %	long
Organic liquids [11]	1 bar / 293 K	10	47 %	long
Metal hydrides [13]	1-3 bar / >293K	15	-	long
Liquid Ammonia [14]	9 bar / 293 K	13	50 %	long

In the case of long-term (months to seasons) storage or in the case of high required capacity, a higher density storage solution is preferable to lower the costs. In that regard, ammonia shows very interesting features (see Table 1). Ammonia is a fuel convenient for storage since it is liquid under 9 bar of pressure and at ambient temperature. It is obtained from hydrogen and air through the Haber-Bosch process, which requires high temperature and pressures (~150 bar, ~400°C) [15]. Liquid ammonia can be produced from electricity, air and water with an efficiency of 50% (LHV) for systems combining a conventional electrolyser to a Haber-Bosch process [14-16]. Under research are the Solid Oxide Electrolysers (SOE) that realises the

electrolysis of water and produces high temperature heat that can be recovered by the Haber-Bosch process for an estimated overall efficiency for the production of liquid ammonia higher than 62% LHV [17,18]. Therefore, the industrial production of liquid ammonia from electricity, air and water can be energetically competitive to other hydrogen storage technologies. Moreover, taking into account the liquid state, non-leaking, energetic density and sustainable properties of ammonia, its high potential as a long-term storage fuel and future energy vector must be acknowledged [19].

Having a dual-fuel storage system (i.e. ammonia and hydrogen), a technology able to use both of them to produce back electricity when needed is required. Moreover, a technology able to perform cold and quick starts would ensure more reliability to the whole electricity system. The piston engine being multifuel (to some extent), a mature technology as backup generator, and low cost (a parameter of primary importance when dealing with renewable energy storage), it shows great potential for such application. Moreover, piston engines are suited for Combined Heat and Power (CHP) applications hence allowing for a higher overall efficiency.

Previous work

Several Spark-Ignition (SI) and Compression-Ignition (CI) engines have been operated in the past decades with ammonia. Still, ammonia having a low flame speed and a high auto-ignition resistance, combustion promoters like gasoline, diesel or hydrogen were used [20, 21, 22, 23]. The high resistance of ammonia to auto-ignition has been used by Duynslaegher et al. to successfully operate a pure ammonia SI engine with compression ratios higher than 13:1, allowing for brake efficiencies of about 39% [24]. Yet, only a poor combustion of ammonia was obtained and such compression ratios do not allow the use of hydrogen in SI engines. Therefore, to meet the goal of a clean and highly efficient ammonia-hydrogen-CHP system, the authors decided to experimentally investigate the use of HCCI combustion. HCCI combustion allow high compression ratios together with low in-cylinder temperatures (no thermal-NO_x) while being inherently multifuel. The multifuel capability of HCCI engines has been demonstrated in several studies [25, 26, 27] and the specific case of both hydrogen and ammonia has been investigated by the authors in a previous study [28].

For a naturally aspirated engine with a compression ratio of 16:1, the authors showed in [28] that the required intake temperatures to have proper combustion timing for hydrogen and ammonia are 440K and 610 K, respectively. Such difference in auto-ignition resistance is linked to their respective ignition delays, see Figure 1.
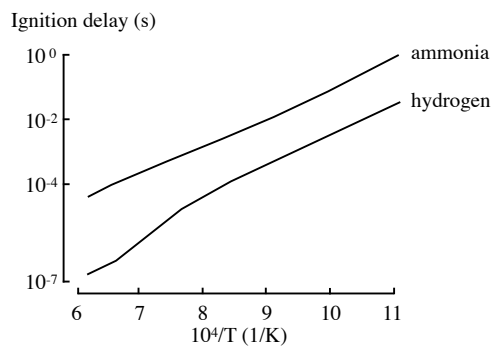

Figure 1. Ignition delays for hydrogen and ammonia in a 0.4 equivalence ratio air-fuel mixture at 50 bar initial pressure, in a constant volume adiabatic chamber. Reproduced from [28].

To the best of our knowledge, ammonia has never been used in HCCI engines except for one unique experiment: Van Blarigan experimented pure ammonia combustion in a 40:1 compression ratio HCCI free piston engine without preheating [29]. The success of this pure ammonia HCCI engine ought solely to the very high compression ratio. Still, such compression ratio cannot be used in the present study for two reasons: (1) the friction losses due to higher pressures would significantly deteriorate the overall efficiency and (2) the engine has to be able to run with pure hydrogen without ringing. Ringing occurs in HCCI engines when the combustion intensity is too high. Even though it occurs through a slightly different mechanism than SI knock (a local auto-ignition inducing a gas expansion at the speed of sound [30, 31]), the consequences are similar. Ibrahim et al. observed a 16:1 compression ratio, naturally aspirated, hydrogen HCCI engine experiencing ringing with equivalence ratios higher than 0.3 [32]. This equivalence ratio limit was shown to decrease linearly with increasing compression ratio [33]. Therefore, to have an engine able to use both fuels efficiently, a trade-off between a high compression ratio to promote ammonia combustion and a limited compression ratio to prevent hydrogen from ringing is needed.

Present work

In the considered dual-fuel storage context, an engine able to operate under different blending ratios of the two fuels would be very desirable. Therefore this paper aims to investigate the effects of a substantial addition of ammonia into hydrogen HCCI combustion. From the literature it appears clearly that there is a lack of knowledge in ammonia combustion under HCCI conditions. Consequently, the achievable ammonia content in a hydrogen HCCI engine is unknown as well as its effect on engine performances and pollutant emissions.

For ammonia combustion under HCCI conditions, the required intake temperature for the auto-ignition to occur is so high that it causes three issues: (1) it is not easy to provide such intake condition and (2) it increases the heat losses and (3) it reduces the mixture density, and consequently the volumetric efficiency. Therefore, the effect of an increased intake pressure to promote ammonia auto-ignition will be assessed. Moreover, the ignition delay of ammonia being really high, the combustion efficiency and combustion duration will be investigated as the ammonia content is increased.

Finally, ammonia and hydrogen being carbon-free molecules, the only concern for fuel emissions will be related to NO_x. Hydrogen combustion under HCCI conditions is usually NO_x-free. Indeed, as it is a low temperature combustion process, the Zeldovich mechanism is irrelevant and no thermal-NO_x are emitted. Nonetheless, when adding ammonia to the mixture, nitrogen radicals will spontaneously appear from ammonia combustion. Therefore fuel-NO_x will be produced. Usual temperature reduction techniques will be helpless as they only influence thermal-NO_x emissions. High EGR rates will be performed to evaluate the oxygen availability impact on fuel-NO_x formation from ammonia combustion.

Methodology

Experimental apparatus

Table 2 gives the specifications of the engine used for the experiments. It is a PSA DW10 engine retrofitted to a single-cylinder engine operating under HCCI conditions. It has been used for various study on HCCI combustion, see for example [34, 35]. It is coupled to

an electric motor to set the rotational speed (fixed at 1500 RPM in this study).

Table 2. Engine specifications

Engine Model	PSA DW10
Displacement volume, V_c	499 cc/cylinder
Stroke / Bore / Conrod length	88 / 85 / 145 mm
Geometric / effective compression ratio	16:1 / 15.3:1
Intake Valve Closing (CAD)	157 bTDC
Exhaust Valve Opening (CAD)	140 aTDC
Coolant temperature	95°C

A schematic representation of the engine test bench is given in Figure 2. To ensure homogeneous intake conditions, the mixture is first admitted into a 10L intake plenum before entering the engine. The Coefficient of Variation of the Indicated Mean Effective Pressure (CoV$_{IMEP}$) obtained throughout this campaign was continuously below 3%. Five mass flow controllers were necessary to allow the use of both fuels while simulating EGR. The gaseous components were controlled by Brooks 585XS devices offering a precision of +/- 0.7% on the measure and +/- 0.2% on their full range. To allow the use of ammonia, high temperature and/or pressure are necessary. Pressurized intake air was supplied by a compressor and intake pressure was measured in the plenum by a piezo-resistive absolute pressure sensor Kistler 4075A offering an accuracy of 0.3% on its full scale. Maximum air pressure allowed by the compressor is 1.6 bar. Two heaters allow the intake temperature to reach 475 K. Intake temperature is measured in each intake pipe by K thermocouples having a precision of +/- 2 K. In-cylinder pressure is measured by a piezo-electric pressure sensor Kistler 6043A having an accuracy of +/- 2% and recorded every 0.1 CAD. NO$_x$ emissions were measured by an Horiba MEXA 7000.
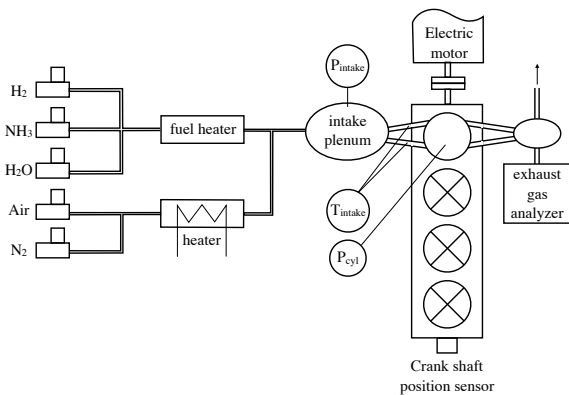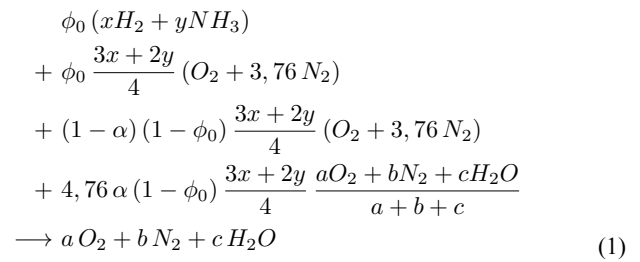

Figure 2. Schematic representation of the experimental apparatus.

Experimental operating conditions

Having an effective compression ratio of 15.3:1 and given the limited test bench intake temperature, pure ammonia operation was not possible. Therefore the HCCI combustion has been studied from full hydrogen to the maximal content in ammonia possible. Moreover, high EGR rate is to be used with ammonia in order to influence the formation of fuel-NO$_x$ through reduced oxygen availability. For each operating condition, the EGR rate, α, is defined as the fraction of excess intake air (compared to stoichiometry) that is replaced by exhaust gases. This will be done experimentally by inserting the

correct amount of nitrogen, oxygen and water vapor before the intake manifold. The general combustion reaction can be written as follows:

$$
\begin{aligned}
&\phi_0 \left(x H_2 + y N H_3 \right) \\
&+ \phi_0 \frac{3x + 2y}{4} \left(O_2 + 3,76\, N_2 \right) \\
&+ (1 - \alpha)(1 - \phi_0) \frac{3x + 2y}{4} \left(O_2 + 3,76\, N_2 \right) \\
&+ 4,76\, \alpha (1 - \phi_0) \frac{3x + 2y}{4} \frac{a O_2 + b N_2 + c H_2 O}{a + b + c} \\
&\longrightarrow a\, O_2 + b\, N_2 + c\, H_2 O
\end{aligned}
\tag{1}
$$

where the second term accounts for the stoichiometric portion of air, the third term is the rest of the intake air that is not replaced by EGR, the fourth term represents EGR replacing the missing mole quantity of intake air and the right hand side of the equation represents the exhaust gases with their respective stoichiometric coefficients a, b, and c. The initial equivalence ratio (without EGR) is noted ϕ_0. All the operating conditions experimented in this work are listed in Table 3.

Table 3. Studied operating conditions and obtained energy content (FuelMEP).

#	Constraint	P_{in} (bar)	H_2 (%vol.)	NH_3 (%vol.)	ϕ	T_{in} (K)	FuelMEP (bar)
1	- Constant blend - Increasing φ	1.5	100	0	0.18 0.19 0.21 0.22 0.24	429	6.7 7.2 7.7 8.2 8.6
2	- Variable blend - Constant CA50 (around 4 CAD) - Increasing φ	1.5	100 68 51 46 42 39	0 32 49 54 58 61	0.21 0.24 0.26 0.26 0.27 0.27	428 439 460 467 474 479	7.7 8.4 8.5 8.5 8.5 8.5
3	- Variable blend - Increasing φ	1.5	47 47 44 38 31	53 53 56 62 69	0.26 0.26 0.27 0.27 0.28	473	8.5 8.5 8.6 8.8 8.8
4	- Variable blend - Constant CA50 (around 4 CAD) - Constant φ	1.5	100 80 67 57 50 46	0 20 33 43 50 54	0.20	428 433 445 458 467 474	7.5 7.2 7.0 6.8 6.6 6.6
5	- Variable blend - Constant T_{in} - Constant φ	1.5	55 50 45 42 40 37 35	45 50 55 58 60 63 65	0.20	473	6.6 6.6 6.5 6.3 6.5 6.5 6.5
6	- Constant blend - Increasing φ	1.0 1.1	100 100	0 0	0.25 0.25 0.26 0.28 0.31 0.22 0.25 0.26 0.28 0.29	428 428	6.0 6.0 6.3 6.7 7.3 6.0 6.7 7.0 7.4 7.7
7	0 % EGR 20 % EGR 40 % EGR 60 % EGR	1.0	80	20	0.30 0.32 0.35 0.40	434 440 451 468	7.0 6.9 6.8 6.6
8	60 % EGR 80 % EGR	1.3	80	20	0.32 0.36	449 470	7.5 6.4

Predictive simulation tool

It is of interest to model ammonia combustion in order to estimate the engine behavior and the required intake conditions for the given experimental engine and operating conditions. To perform these simulations, a 0-Dimensional model has been used. The model, further developed in [28], reproduces the evolution of the in-cylinder thermodynamic state and uses calibrated heat losses so that the estimated combustion onset corresponds to the experimental CA10. This model will be used as well in the present study to investigate specific conditions that the experimental set-up was unable to reach.

To obtain accurate results, the model must be supplied with an appropriate hydrogen-ammonia kinetic mechanism. The mechanism has to be validated for HCCI conditions, i.e. regarding ignition delay, and for high pressure and lean conditions. The chosen hydrogen-ammonia mechanism is the one from Mathieu and Petersen, validated at high pressure (30 bar) and for lean conditions (equivalence ratio of 0.5), and at stoichiometry, in a shock tube [36]. This mechanism is based on the mechanism from Dagaut et al. [37] and focused on improving the ammonia NO_x chemistry from their experiments.

Results and discussion

Resistance to auto-ignition of ammonia

Ammonia has been found to be even more resistant to auto-ignition than expected from the simulations. Figure 3 shows the experimental and simulated required intake temperatures (such that the CA10 occurs close to TDC) for various hydrogen-ammonia blends. The limited test bench intake pressure and temperature did not allow to operate with an ammonia volumetric content higher than 61% (for CA10 occurring at TDC). Above such concentration in ammonia the resistance to auto-ignition increases in an exponential way, as seen from the required intake temperature in Figure 3. This fact highlights the theoretical promoting effect of hydrogen on ammonia.
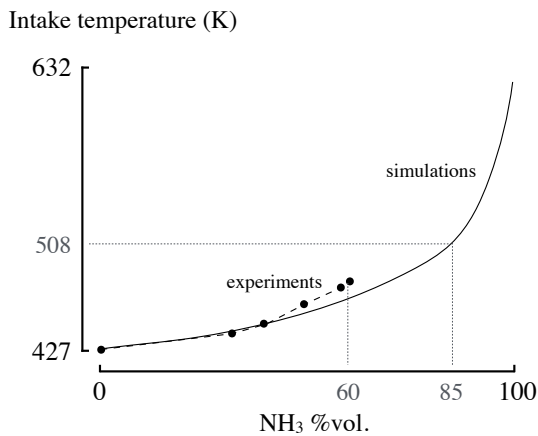
Intake temperature (K)

Figure 3. Experimental and simulated required intake temperatures for various hydrogen-ammonia blends such that the auto-ignition (CA10) occurs close to TDC. Experimental data corresponds to operating conditions # 2. Both ammonia resistance to auto-ignition and hydrogen promotion effect are observable.

Even though the auto-ignition resistance seems to have little effect below 60 %vol. in ammonia content, it induces substantial effects on the combustion timing, as shown in Figure 4 where the pressure

curves obtained for various hydrogen-ammonia blends are displayed. In this case, the intake pressure and temperature have been kept constant (operating conditions # 3). For these four operating points, the CA50 is delayed from 2.1 to 8.0 CAD.
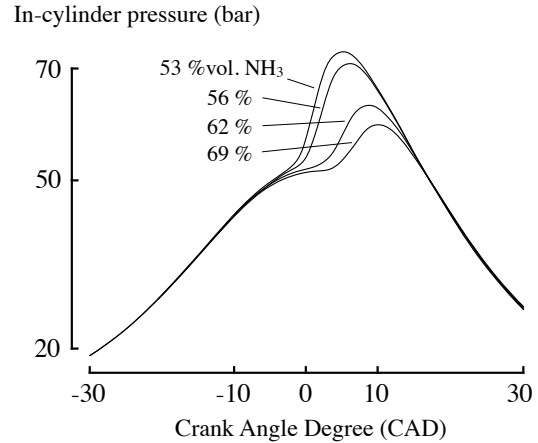
In-cylinder pressure (bar)

Figure 4. Pressure curves for various hydrogen-ammonia blends (operating conditions # 3). The combustion timing is heavily affected by ammonia content.

Ammonia combustion characterization

Allowing the combustion of ammonia by increasing the intake temperature is not sufficient to achieve good performances. Given its very long ignition delay (see Figure 1), it is of interest to reach high in-cylinder temperatures to reduce the probability of unburned gases. Figure 5 displays the combustion efficiency as a function of the maximal in-cylinder temperature. As no exhaust gas measurements were available for unburned hydrogen and ammonia, the Combustion Efficiency (CE) is defined as the ratio between the released heat and the mixture energy content:

$$CE = \frac{\sum_{\theta=-40}^{40} HRR(\theta) \cdot \Delta\theta}{m_{fuel} \cdot LHV_{fuel}} \tag{2}$$

where HRR is the Heat Release Rate (J/CAD) computed from the in-cylinder pressure, which is measured every $\Delta\theta = 0.1$ CAD. The overall low combustion efficiency is due to the inadequate piston shape (conventional Diesel piston shape) and to the non-optimized combustion chamber (high squish volume). Therefore only a qualitative analysis regarding the CE will be performed. Figure 5 highlights the dropping combustion efficiency of ammonia for maximal in-cylinder temperatures lower than 1300 K. Beyond the quenching consideration and wall temperature, this has to do with the ignition delay being highly influenced by the temperature. Still, for pure hydrogen operation, maximal combustion efficiency was maintained below that temperature given its lower ignition delay.
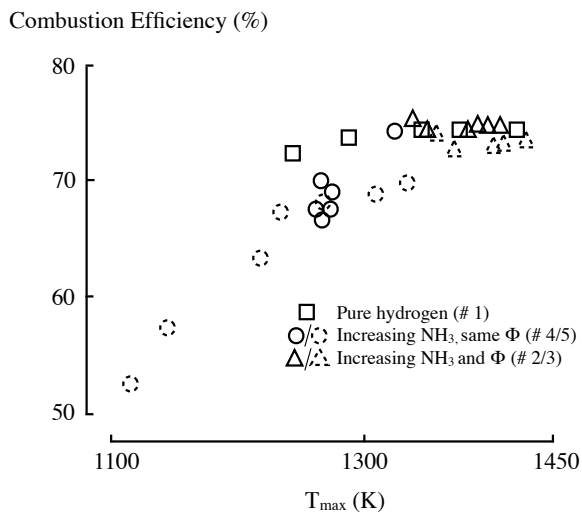
Combustion Efficiency (%)

Figure 5. Combustion efficiency as a function of the maximal in-cylinder temperature for operating conditions # 1,2,3,4,5. Staying higher than 1300 K ensures a good combustion efficiency for ammonia. The overall low combustion efficiency is due to a non-optimized combustion chamber (high squish volume) and piston shape (conventional Diesel piston shape).

To overcome the decrease in combustion efficiency for increasing ammonia proportions, a boost in in-cylinder temperature is necessary. Although ammonia has a higher molar LHV than hydrogen, simply increasing the ammonia proportion (for a constant equivalence ratio) does not produce higher in-cylinder temperatures. Indeed, as the stoichiometric combustion of ammonia requires more air, the FuelMEP will stay more or less constant. For the operating conditions #5, the intake temperature is kept constant and therefore the combustion timing is delayed with increasing ammonia proportions, hence the decrease in maximum in-cylinder temperature and CE. For the operating points #4, the CA50 is kept constant through an increase in intake temperature. Therefore, the decrease in CE is due to the too small in-cylinder temperature that does not trigger ammonia kinetics soon enough in the cycle. However, the maximum in-cylinder temperature can be increased by increasing the fuel quantity inside the cylinder. Operating conditions # 2,3 reproduces the same conditions as # 4,5, excepted that the equivalence ratio is increased as the ammonia proportions increases. Therefore, maximal in-cylinder temperature increases with ammonia, which diminishes the ignition delays for ammonia and allow hydrogen-like CE.

The consequence of the difference in the ignition delay between hydrogen and ammonia can be seen on the heat release rate curves, displayed in Figure 6 for three of the operating conditions # 2. The curves with ammonia are more asymmetric than the one for pure hydrogen. Consequently, the overall heat released can be decomposed in two cumulative events: (1) the combustion of hydrogen which (2) triggers the combustion of ammonia, following their respective ignition delays. Still, looking at the HRR curves, these two events overlap: the onset of hydrogen combustion will occur first and then, helped by the increase in temperature and the presence of radicals, the ammonia combustion will be triggered. The slower increase in HRR for the cases containing ammonia is due to a decrease in hydrogen mixture concentration.
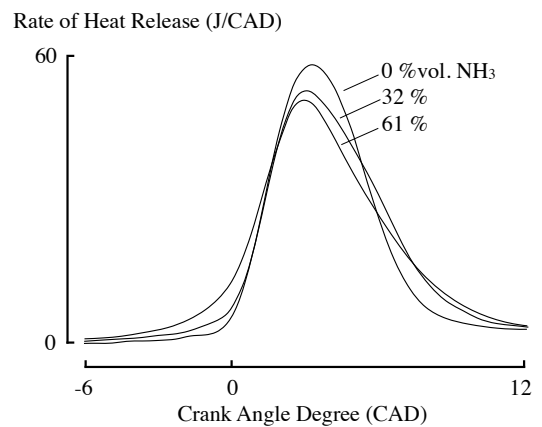
Rate of Heat Release (J/CAD)

Figure 6. Rate of Heat Release curves for various hydrogen-ammonia blends of the operating condition # 2. The asymmetry of the ammonia containing curves indicates cumulative combustion events of the hydrogen and the ammonia contained in the cylinder..

These cumulative combustion events translate into an overall increased combustion duration. Figure 7 displays the influence of ammonia content on the combustion duration for the operating conditions # 2,4. For both cases the combustion duration increases with the ammonia proportion. The effect is so strong that the equivalence ratio of the operating conditions #2 can be increased from 0.21 to 0.27 without increasing the maximum HRR (see Figure 6).
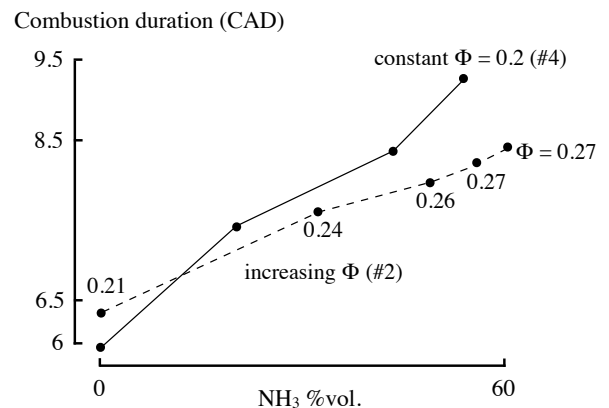
Combustion duration (CAD)

Figure 7. Combustion duration as a function of the ammonia mixture content for operating conditions # 2,4. Increasing ammonia contents induce longer combustions. In operating conditions # 2, even though the fuel content is increased as the ammonia content is increased, the combustion duration increases.

Ringing behavior of hydrogen and ammonia

The power output of hydrogen HCCI engines is restricted due the limited equivalence ratios used to avoid ringing. The easiest way to reduce hydrogen ringing for a given equivalence ratio is to delay its combustion later in the cycle to enforce a longer combustion duration. Yet, this solution leads to a non optimal cycle and it is therefore not ideal for extended operation times. In the considered configuration, the longer combustion duration for hydrogen-ammonia blends can be exploited to reduce the ringing issues related to hydrogen. Moreover, as the ringing results in resonating in-cylinder pressure waves, studies have shown the interest of increasing the in-

cylinder pressure to diminish the intensity contained in the pressure waves and hence to decrease ringing intensity [30,31]. These two points have been studied and the results are described below.

Figure 8 displays the ringing intensity and FuelMEP the operating conditions #1,2,4,6 against Maximum Pressure Rise Rate (MPRR). The ringing intensity of a combustion cycle is defined as the maximal amplitude of the pressure signal (in bar) filtered between 4 kHz and 25 kHz [30,31]. The ringing intensity given here is the average of the maximal amplitudes obtained for 100 consecutive combustion cycles. The measurement noise for the ringing intensity is in the order of 0.1 bar. Above that point, a correlation between ringing intensity and MPRR for the four operating conditions can be clearly seen. Moreover, by evaluating the noise produced by the engine, a ringing limit was set to 0.15 bar of ringing intensity and therefore a MPRR limit was set to 5.5 bar/CAD. Consequently, two results can be drawn from the evolution of the FuelMEP as a function of the MPRR. Firstly, by comparing operating conditions # 1,6 for pure hydrogen, it can be seen that for an identical MPRR, the condition with a higher intake pressure allows a higher FuelMEP. Therefore increasing the intake pressure allows to increase the energy content inside the cylinder while avoiding ringing, hence a higher Brake Mean Effective Pressure (BMEP). Secondly, looking at the operational conditions # 2,4 shows the combined effect of ammonia and equivalence ratio. For the operating condition # 4, as the ammonia proportion is increased the MPRR decreases. However, for the operating conditions # 2, even though the equivalence ratio is increased compared to operating conditions # 4, the MPRR still decreases as a result from the cumulative combustion events and the lengthening of the combustion duration. Therefore these cumulative combustion events, a characteristic of the hydrogen-ammonia blends, allows an un-correlation between the FuelMEP and the MPRR and consequently allows for high power densities in the ringing-safe region.

Figure 8. Ringing intensity and FuelMEP as a function of MPRR. Ringing and MPRR are shown to be correlated. An increased intake pressure allows higher FuelMEP for the same MPRR and ammonia presence reduces the MPRR for the same FuelMEP.

Keeping only the ringing-safe operating points for the conditions # 1,2,4, the obtained IMEP as a function of the FuelMEP is displayed in Figure 9. The obtained IMEP is higher for the ammonia containing cases given their higher allowed FuelMEP. Yet, a smaller efficiency is observed as the ammonia content increases. Indeed, for the operating condition #2 the CA40 is kept constant by increasing the intake temperature hence a higher heat loss. For operating condition #4, the efficiency is fairly maintained as the ammonia content increases with a constant intake temperature.
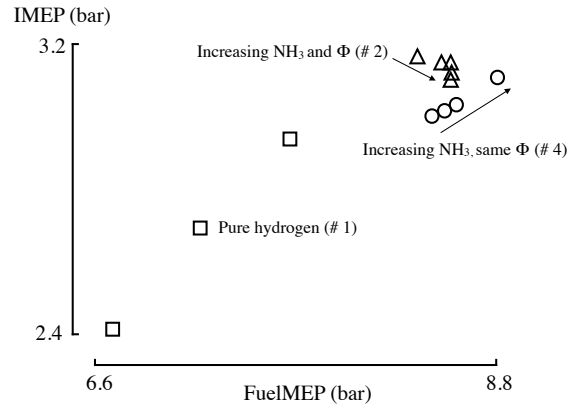

Figure 9. IMEP as a function of the FuelMEP for the ringing-safe operating conditions # 1,2,4. With an increasing ammonia content, depending on the increased intake temperature (#2) or constant intake temperature (#4), the gross efficiency decreases or stays constant, respectively.

For non-carbonated fuels like hydrogen and ammonia, no PM, HC or CO can be emitted from the combustion of the fuel. The only pollutants of concern here are NO_x. For pure hydrogen conditions, the measured NO_x emissions were constantly below 6 ppm. Indeed, the data post processing revealed overall maximal in-cylinder temperature in the order of 1400 K, well below the thermal-NO_x limit of 1800 K. Yet, as soon as some ammonia was added in the mixture, a surge of NO_x emissions above several thousands ppm was observed, see Figure 10, whereas the global in-cylinder temperature did not increase. Therefore these emissions are not linked to the thermal route but they find their origins in the nitrogen contained in ammonia, which is set free as soon as the combustion starts. A decrease in NO_x emissions can be seen in Figure 10 with an increase in ammonia proportion. No factual proof could be brought for this observation, although the authors believe it is linked to an increased ammonia concentration in the exhaust gases. Indeed, as the ammonia proportion at the intake increases, the unburned ammonia concentration increases. Consequently, either the measurement method (chemiluminescence) was flawed because of the ammonia content in the sampled gases, or some Selective Non-Catalytic Reduction (SNCR) took place during the expansion stroke. Indeed, chemiluminescence for NO_x measurement has already been shown to be affected by ammonia presence [38] and SNCR is known to happen in presence of ammonia and NO_x at temperatures around 700 K [39], as during the expansion stroke. It is to be noted that both phenomenon can have occurred.
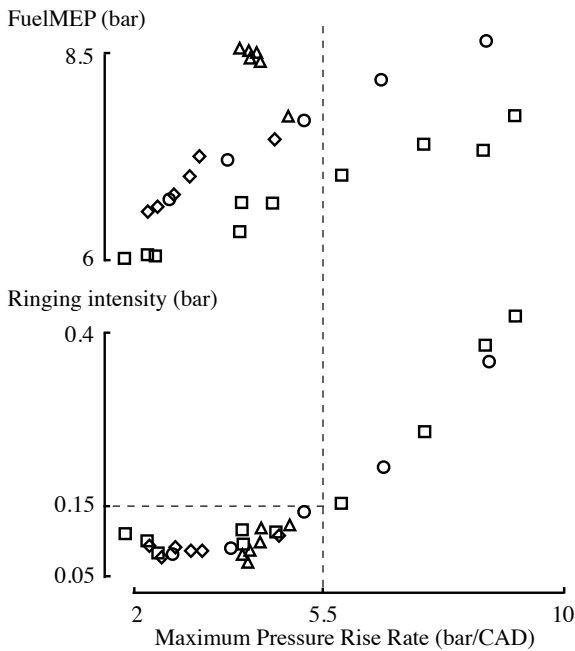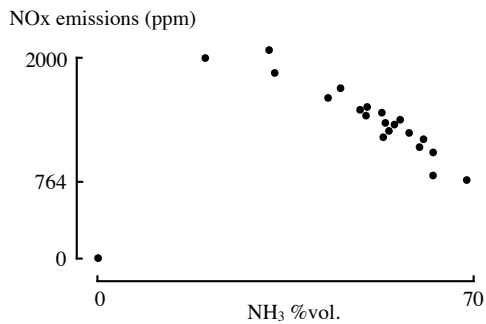
NOx emissions (ppm)

Figure 10. Measured NO_x emissions as a function of the ammonia mixture content for operating conditions # 2,3,4,5. NO_x emissions are smaller than 6 ppm for pure hydrogen combustion and are in the order of 1000 to 2000 ppm as soon as some ammonia is added in the mixture.

As explained in the introduction, EGR can be used to reduce the oxygen excess and hence penalize the incomplete combustion pathway of ammonia. Figure 11 displays the NO_x emissions against various EGR rates, for the set of experiments # 3,4. The absolute values cannot be compared between the two set of experiments as they were done with different equivalence ratios, different intake pressures and different CA50. But the decreasing trend of NO_x emissions with an increase in EGR rate is significant. The maximal in cylinder temperature staying approximately constant with the varying EGR, the reduced NO_x production can be attributed to the reduced oxygen availability.
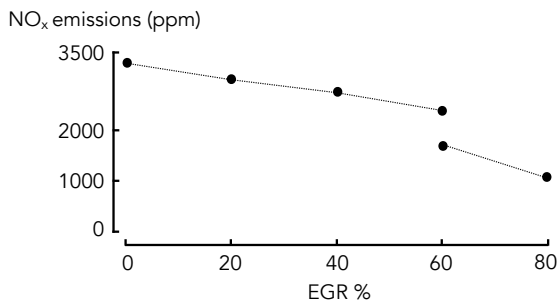

Figure 11. NO_x emissions as a function of the EGR rate for the operating condition # 7,8. Reduced oxygen availability reduces the formation of NO_x.

Unfortunately the evaporator used to produce the steam of the synthetic EGR was not powerful enough to evaporate the water flow needed to simulate a 100 % EGR. Theoretically, very few fuel-NO_x would be produced in such conditions as barely no excess oxygen would be available. This effect has been verified through the simulation (with the 0D model developed in [28]) of the operating conditions #7 with up to 100% EGR, see Figure 12. The simulated results give a similar response to EGR as the experiments. With full EGR the fuel-air mixture was at stoichiometry, therefore the NO emissions were reduced to 89 ppm (no NO2). However, the production of N_2O (strong greenhouse gas) was forecasted by the model, on which EGR had only a limited effect. Still, this point has to be verified experimentally because of the limited combustion representativity of a 0D model. Moreover, an impact on the combustion efficiency should be expected with such high rates of EGR. Indeed, for the operating condition # 7, two percentage points of combustion efficiency were lost when going from no EGR to 60% EGR. Therefore, the use of high EGR rates does not seem to be an effective solution as an after-treatment system would still be required for N_2O emissions.
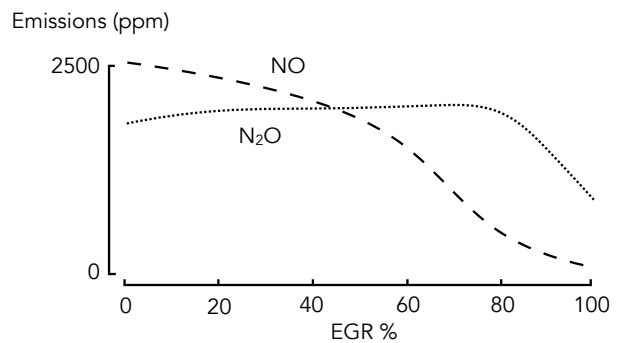
Emissions (ppm)

Figure 12. 0D simulations of the production of NO and N_2O for the operating condition # 7. Going towards stoichiometric conditions allows to reduce the NO_x production to 89 ppm but the N_2O production is still substantial.

Findings and Conclusions

A 15.3:1 effective compression ratio HCCI engine has been used to burn various hydrogen-ammonia blend ratios. Using the maximal achievable intake pressure (1.5 bar) and the maximal intake temperature (475 K), the engine was able to operate with an ammonia content up to 70 %vol. Given the very high ignition delay of ammonia, in-cylinder temperatures need to stay above 1300 K to maintain hydrogen-like combustion efficiencies. Cumulative (i.e. overlapping) combustion events were observed for hydrogen-ammonia blends leading to longer combustion durations. This effect allowed to increase the FuelMEP compared to pure hydrogen while staying in ringing-safe operations. The reducing ringing intensity effect of an increased intake pressure was also verified. Finally, NO_x emissions originating from the fuel were obtained for ammonia containing blends. Although NO_x emissions could be significantly reduced through the use of massive EGR (with a certain cost on combustion efficiency), simulations showed that N_2O emissions were produced as well and unaffected by EGR. The main conclusions of this paper regarding the findings are :

- Higher compression ratios and intake pressure should be used with ammonia in order to minimize the required intake temperature and hence maximize the IMEP and efficiency. However, the hydrogen tendency for ringing with high compression ratio would be an issue. This demonstrates the advantage that a variable compression ratio engine would represent for this dual fuel cogeneration system.

- Blending hydrogen and ammonia helps increasing the power density (by increasing combustion duration) and therefore could lead to enhanced brake efficiencies through smaller relative mechanical and heat losses.

- Full EGR could theoretically be used to cancel fuel-NO_x emissions. Still, it would require strategies to compensate for the induced loss in combustion efficiency and the use of a SCR system would be required to eliminate the N_2O production.

Future work will be focused on the precise emissions measurements of unburned hydrogen and ammonia, and of NO_x and N_2O. Moreover, the use of a heavy duty engine allowing for a pure ammonia content is of interest.

References

1. Rodriguez, R. A., Becker, S., Andresen, G.B., Heide, D., et al., "Transmission needs across a fully renewable European power system," Renewable Energy, vol. 63, pp. 467–476, 2014. doi: 10.1016/j.renene.2013.10.005.

2. Hedegaard, K. and Meibom, P., "Wind power impacts and electricity storage - A time scale perspective," Renewable Energy, vol. 37, pp. 318–324, 2012. doi: 10.1016/j.renene.2011.06.034.

3. Akinyele, D. and Rayudu, R., "Review of energy storage technologies for sustainable power networks," Sustainable Energy Technologies and Assessments, vol. 8, pp. 74–91, 2014. doi: 10.1016/j.seta.2014.07.004.

4. Bussar, C., Stöcker, P., Cai, Z., Moraes, L. J., et al., "Large-scale integration of renewable energies and impact on storage demand in a European renewable power system of 2050 Sensitivity study," Journal of Energy Storage, vol. 6, pp. 1–10, 2016. doi: 10.1016/j.est.2016.02.004.

5. Yekini, M., Wazir, M. and Bashir, N., "Energy storage systems for renewable energy power sector integration and mitigation of in- termittency," Renewable and Sustainable Energy Reviews, vol. 35, pp. 499–514, 2014. doi: 10.1016/j.rser.2014.04.009.

6. Diaz-gonzalez, F., Sumper, A., Gomis-bellmunt, O. and Villafafila-robles, R., "A review of energy storage technologies for wind power applications," Renewable and Sustainable Energy Reviews, vol. 16, no. 4, pp. 2154–2171, 2012. doi: 10.1016/j.rser.2012.01.029.

7. Walker, S. B., Mukherjee, U., Fowler, M. and Elkamel, A. "Benchmarking and selection of Power-to-Gas utilizing electrolytic hydrogen as an energy storage alternative," International Journal of Hydrogen Energy, vol. 41, no. 19, pp. 7717–7731, 2016. doi: 10.1016/j.ijhydene.2015.09.008.

8. Jülch, V., "Comparison of electricity storage options using levelized cost of storage (LCOS) method," Applied Energy, vol. 183, pp. 1594–1606, 2016. doi: 10.1016/j.apenergy.2016.08.165.

9. Klumpp, F., "Comparison of pumped hydro, hydrogen storage and compressed air energy storage for integrating high shares of renewable energies Potential , cost-comparison and ranking," Journal of Energy Storage, vol. 8, pp. 119–128, 2016. doi: 10.1016/j.est.2016.09.012.

10. Gardiner, M., "Energy requirements for hydrogen gas compression and liquefaction as related to vehicle storage needs," tech. rep., DOE Department OF Energy, 2009.

11. Wang, H., Zhou, X. and Ouyang, M., "Efficiency analysis of novel Liquid Organic Hydrogen Carrier technology and comparison with high pressure storage pathway," International Journal of Hydrogen Energy, vol. 41, pp. 18062–18071, 2016. doi: 10.1016/j.ijhydene.2016.08.003.

12. Teichmann, D., Arlt, W. and Wasserscheid, P., "Liquid Organic Hydrogen Carriers as an efficient vector for the transport and storage of renewable energy," International Journal of Hydrogen Energy, vol. 37, no. 23, pp. 18118–18132, 2012. doi: 10.1016/j.ijhydene.2012.08.066.

13. Aslam, R., Muller, K., Muller, M., Koch, M., et al., "Measurement of Hydrogen Solubility in Potential Liquid Organic Hydrogen Carriers," Journal of chemical & engineering data, vol. 61, pp. 643–649, 2015. doi: 10.1021/acs.jced.5b00789.

14. Morgan, E.R., "Techno-Economic Feasibility Study of Ammonia Plants Powered by Offshore Wind," University of Massachusetts, dissertation, Tech. Rep., 2013. http://scholarworks.umass.edu/open access dissertations/697

15. European Commission, "Best Available Techniques for the Manufacture of Large Volume Inorganic Chemicals - Ammonia, Acids and Fertilisers," Tech. Rep. August, European Commission - Integrated Pollution Prevention and Control, 2007.

16. Fuhrmann, J., Hülsebrock, M. and Krewer, U., Transition to Renewable Energy Systems - Energy Storage Based on Electrochemical Conversion of Ammonia. Wiley-VCH Verlag GmbH & Co. KGaA, 1st ed., 2013.

17. G. Cinti, D. Frattini, E. Jannelli, U. Desideri, and G. Bidini, "Coupling Solid Oxide Electrolyser (SOE) and ammonia production plant," Applied Energy, vol. 192, pp. 466–476, 2017. doi: 10.1016/j.apenergy.2016.09.026

18. ISPT, "Power to Ammonia," Tech. Rep., 2016. http://www.ispt.eu/media/ISPT-P2A-Final-Report.pdf.

19. Ahlgren, W. L., "The Dual-Fuel Strategy: An Energy Transition Plan," Proceedings of the IEEE, vol. 100, no. November 11, 2012.

20. Frigo, S. and Gentili, R., "Analysis of the behaviour of a 4-stroke Si engine fuelled with ammonia and hydrogen," International Journal of Hydrogen Energy, vol. 38, pp. 1607–1615, 2013. doi: 10.1016/j.ijhydene.2012.10.114.

21. Grannell, S., Assanis, D., Bohac, S. and Gillespie, D., "The Operating Features of a Stoichiometric, Ammonia and Gasoline Dual Fu- eled Spark Ignition Engine," in ASME 2006 International Mechanical Engineering Congress and Exposition, vol. 13048, (Chicago, Illinois, USA).

22. Reiter, A. J. and Kong, S.-C., "Demonstration of Compression-Ignition Engine Combustion Using Ammonia in Reducing Green- house Gas Emissions," Energy & Fuels, vol. 22, pp. 2963–2971, 2008. doi: 10.1021/ef800140f.

23. Koike, M., Miyagawa, H., Suzuoki, T. and Ogasawara, K. "Ammonia as a hydrogen energy carrier and its application to internal combustion engines," in Sustainable Vehicle Technologies, Driving the green agenda, pp. 61–70, Gaydon, UK: WoodHead Publishing, institutio ed., 2012.

24. Duynslaegher, C., Experimental and numerical study of ammonia combustion. PhD thesis, Université Catholique de Louvain, 2011.

25. Christensen, M., Johansson, B., Amneus, P. and Mauss, F., "Super- charged Homogeneous Charge Compression Ignition,"

SAE Technical Paper 1999-01-3679, 1998. doi: 10.4271/1999-01-3679

26. Jeuland, N., Montagne, X. and Duret, P., "New HCCI / CAI Combustion Process Development : Methodology for Determination of Relevant Fuel Parameters," Oil & Gas Science and Technology, vol. 59, no. 6, pp. 571–579, 2004. doi: 10.2516/ogst:2006006x.

27. Tanaka, S., Ayala, F., Keck, J. C. and Heywood, J. B., "Two-stage ignition in HCCI combustion and HCCI control by fuels and additives," Combustion and Flame, vol. 132, no. 1-2, pp. 219–239, 2003. doi: 10.1016/S0010-2180(02)00457-1.

28. Pochet, M., Dias, V., Jeanmart, H., Verhelst, S., et al., "Multifuel CHP HCCI engine towards flexible power-to-fuel : numerical study of operating range," Energy Procedia, 2016. doi: 10.1016/j.egypro.2017.03.468.

29. Van Blarigan, P., "Advanced Internal Combustion Engine Research," in 2000 U.S DOE Hydrogen Program Review, (San Ramon, California), pp. 639–656, 2000.

30. Yelvington, P. E. , Design of a Viable Homogeneous-Charge Compression-Ignition (HCCI) Engine : A Computational Study with Detailed Chemical Kinetics. PhD thesis, Massachusetts Institute of Technology, 2004.

31. Eng, J. A., "Characterization of Pressure Waves in HCCI Combustion," SAE Technical Paper 2002-01-2859, 2002. doi: 10.4271/2002-01-2859.

32. Mohamed Ibrahim, M. and Ramesh, A., "Investigations on the effects of intake temperature and charge dilution in a hydrogen fueled HCCI engine," International Journal of Hydrogen Energy, vol. 39, no. 26, pp. 14097–14108, 2014. doi: 10.1016/j.ijhydene.2014.07.019.

33. Lee, K. J., Kim, Y. R., Byun, C. H. and Lee, J. T., "Feasibility of compression ignition for hydrogen fueled engine with neat hydrogen-air pre-mixture by using high compression," International Journal of Hydrogen Energy, vol. 38, no. 1, pp. 255–264, 2013. doi: 10.1016/j.ijhydene.2012.10.021.

34. Contino, F., Foucher, F., Mounaïm-Rousselle, C. and Jeanmart. H., "Experimental characterization of ethyl acetate, ethyl propionate, and ethyl butanoate in a homogeneous charge compression ignition engine," Energy & Fuel, 25(3):998–1003, 3 2011. doi: 10.1021/ef101602q.

35. Dubreuil, A., Foucher, F., Mounaïm-Rousselle, C., "Effect of EGR chemical components and intake temperature on HCCI combustion development," SAE technical paper 2006-32-0044, 2006, doi: 10.4271/2006-32-0044.

36. Mathieu, O. and Petersen, E. L., "Experimental and modeling study on the high-temperature oxidation of Ammonia and related NOx chemistry," Combustion and Flame, vol. 162, pp. 554–570, 2015. doi: 10.1016/j.combustflame.2014.08.022.

37. Dagaut, P., Glarborg, P. and Alzueta, M. U., "The oxidation of hydrogen cyanide and related chemistry," Progress in Energy and Combustion Science, vol. 34, pp. 1–46, 2008. doi: 10.1016/j.pecs.2007.02.004.

38. Hoard, J., Snow, R., Xu, L., Hammerle, R., et al., "NOx Measurement Errors in Ammonia-Containing Exhaust," in Diesel Engine Emissions Reduction Meeting, (Detroit), pp. 1–29, 2006.

39. von der Heide, B., "SNCR Process - Best Available Technology for NOx Reduction in Waste To Energy Plants," in Power-Gen Europe, no. June, (Milan), 2008.

Contact Information

Maxime Pochet - FRIA fellow

Institut de Mécanique, Matériaux et Génie Civil (iMMC)
Université Catholique de Louvain, Belgium
Place du levant 2, 1348 Louvain-la-Neuve, Belgium
max.pochet@uclouvain.be
Tel +32 10 47 22 20

Department of Mechanical Engineering (MECH)
Vrije Universiteit Brussel, Belgium
maxime.pochet@vub.be

BURN joint research group
Vrije Universiteit Brussel & Université Libre de Bruxelles
www.burn-research.be

Acknowledgments

Definitions/Abbreviations

BMEP   Brake Mean Effective Pressure

CA10   Crank Angle at which 10% of the combustion heat has been released

CA50   Crank Angle at which 50% of the combustion heat has been released

CAD   Crank Angle Degree

CAPEX   Capital Expenditure

CE   Combustion Efficiency

CHP   Combined Heat and Power

CI   Compression Ignition

CoV$_{IMEP}$ Coefficient of Variation of the IMEP

EGR   Exhaust Gas Recirculation

FuelMEP   Fuel Mean Effective Pressure

HC   Hydro-Carbons

HCCI   Homogeneous-Charge Compression-Ignition

HRR   Heat Release Rate

IMEP   Indicated Mean Effective Pressure

LHV   Lower Heating Value

MPRR   Maximum Pressure Rise Rate

PM   Particulate Matter

SI   Spark Ignition

SNCR   Selective Non-Catalytic Reduction

TDC   Top Dead Center

α EGR rate

ϕ Equivalence ratio

ϕ_0 Equivalence ratio without EGR